Silicon (2020) 12:413–423
https://doi.org/10.1007/s12633-019-00148-y

ORIGINAL PAPER

Air Jet Erosion Studies on Mg/SiC Composite

K. Balamurugan[1] · M. Uthayakumar[2] · M. Ramakrishna[1] · U. T. S. Pillai[3]

Received: 20 December 2018 / Accepted: 20 March 2019 / Published online: 2 April 2019

Abstract
Magnesium with 10% SiC is identified to be a suitable composition for wear resistance application. To improve the utilization of this composite for various industrial applications, erosion study has been conducted by using air jet erosion tester with varied machining conditions. The composite is prepared by a conventional stir casting process. Alumina is taken as an erodent particle. Impact angle, erosion velocity, and discharge rate are taken as the governing parameters of erosion rate. Lower impact angle and high erodent velocity yield to have a high erosion rate of 0.022 g/min with the least surface finish of 1.48 μm. Erosion velocity is found to have a significant effect of 59% over the other considered parameters. Further, the analysis of the surface profile parameters likely; Ssk, Sku, Sp, Sv, and Sa on the machined surface reveals the mechanism of the material removal and also, the surface defects are analyzed by using SEM image.

Keywords Mg/SiC composite · Air jet erosion · Impact angle · Erodent velocity · Surface profile

Nomenclature

IA	Impact angle
EV	Erodent velocity
DR	Discharge rate
Er	Erosion rate
Ssk	Skewness
Sku	Kurtosis
Sp	Maximum peak height
Sv	Maximum valley depth
SEM	scanning electron microscopy
VHN	Vickers hardness number

1 Introduction

Magnesium is proven to be suitable replacement material for aluminium because of its low density, superior strength-weight ratio, and excellent mechanical properties. To enhance the utilization of magnesium for various engineering applications, ceramic particles are added as reinforcement. Viswanath et al. [1] fabricated Mg composite with the varied composition of SiC through stir casting process and achieved an even dispersion of SiC particles even at 25% composition in the matrix. According to Kumar et al. [2], Mg + 10% of SiC has the excellent wear resistance property. However increase of SiC reinforcement in the matrix increases the wear resistance property simultaneously, it also increases the hardness and density of the composite. Viswas et al. [3] noted similar observation like a decrease in erosion rate on increase at SiC in Al6061/tungsten chromium nickel composite.

Gousia et al. [4] observed different types of wear mechanism on the aluminum-based composite with a change in impact angle by solid particle erosion test. Patel et al. [5] studies on air jet erosion concluded that low impact angle improves the erosion rate on SS 304 and tends to form plastic deformation surfaces with the formation of crater and lips. Whereas the controversy report was given by Sharma et al. [6] that, the erosion rate increases with an increase in the nozzle angle from 30° to 90°, while on machining the hard WC material. From the above survey, it is confirmed that the erosion property differs with the property of the materials irrespective of its machining conditions.

Khan et al. [7], observed an increase in hardness of the composite with increase of SiC reinforced in Zinc based composite. According to Mamatha et al. [8], SiC reinforced Zn found to have low erosion loss and the study is concluded as the addition of SiC in Zn enhances the erosion wear rate rather than Al/SiC

✉ M. Uthayakumar
uthaykumar@gmail.com

[1] Department of Mechanical Engineering, VFSTR (Deemed to be University), Guntur, AP, India

[2] Faculty of Mechanical Engineering, Kalasalingam University, Krishnankoil 626 126, India

[3] Material Science and Technology Division, CSIR – National Institute for Interdisciplinary Science and Technology, Thiruvananthapuram 695019, India

composite. Chowdhury et al. [9] reported that minimum impingement angle and high stand-off distance will have a low erosion rate. The highest hardness value shows the lower erosive and wears rate with micro ploughing surface distortion. Rosa et al. [10] designed an experimental setup with a swing motion nozzle. Through the observation, it is concluded that the erosion rate is found to be high in the non-swing mode particularly at a low impact angle. From this study, it can be stated that the erosion rate of any materials could be effectively measured using the fixed nozzle condition itself. Khan and Dixit [11] observed that removal of materials under erosion test will exercise corrosive, erosion and abrasion type of wear mechanism. Miyazaki [12] had made a critical review on the solid particle erosion on polymer matrix composite, metal matrix composite and ceramic matric composite stated that there is no critical finding had been reported regarding the matrix composition so far.

Yang et al. [13] has found that in erosion test, environmental temperature plays a significant role on determining the machiniability of the materials. In particular for Iron-Sailon composite experienced low erosion rate at both the low and extreme temperature conditions (here temperaturing conditions denote the temperature at which samples are machined) leads to have low erosion rate whereas medium temperature results in excess removal materials. Ruslan and Fengzhou [14] discussed on the thermal effect caused by solid erodent particle on erosion test which will lead to raise the surface temperature of the sample. It has produced a small metal coating on the machined area and the generated thermal energy were dissipated into the subsurface of the sample which create several microcracks and progess to surface defect. Krolczyk et al. [15] performed the machining operations like turning, milling, planning and grinding operation where Krolczyk et al. [16] performed turning operation alone with the dry and wet condition. The surface topography of the samples is studied by considering the various surface profile parameters like Ssk, Skq, Sp, Sv, and Sa and suggested that these parameters are more sensitive to local peaks and valleys and far better in describing the surface texture.

In this study, Mg/SiC composite has excellent wear resistance property with low hardness and density, respectively are prepared by conventional stir casting process under argon atmosphere. Over the entire experimental observations, alumina is used as an erodent material. The influencing parameter in air jet erosion such as Impact Angle (IA), Erodent Velocity (EV) and Discharge Rate (DR) are taken as the governing parameters of Erosion rate (Er). Machining effects and its parameter contribution on output response, the surface profile parameter analysis, and surface morphological studies along with the hardness on the machined surface are discussed. To improve the utilization of this composite for automobiles and piping industries, this erosion study observation will be as a database for their future manufacturing.

2 Materials and Methods

2.1 Material Preparation

Mg + 10% SiC, an excellent wear resistance composite is successfully prepared through a conventional stir casting process

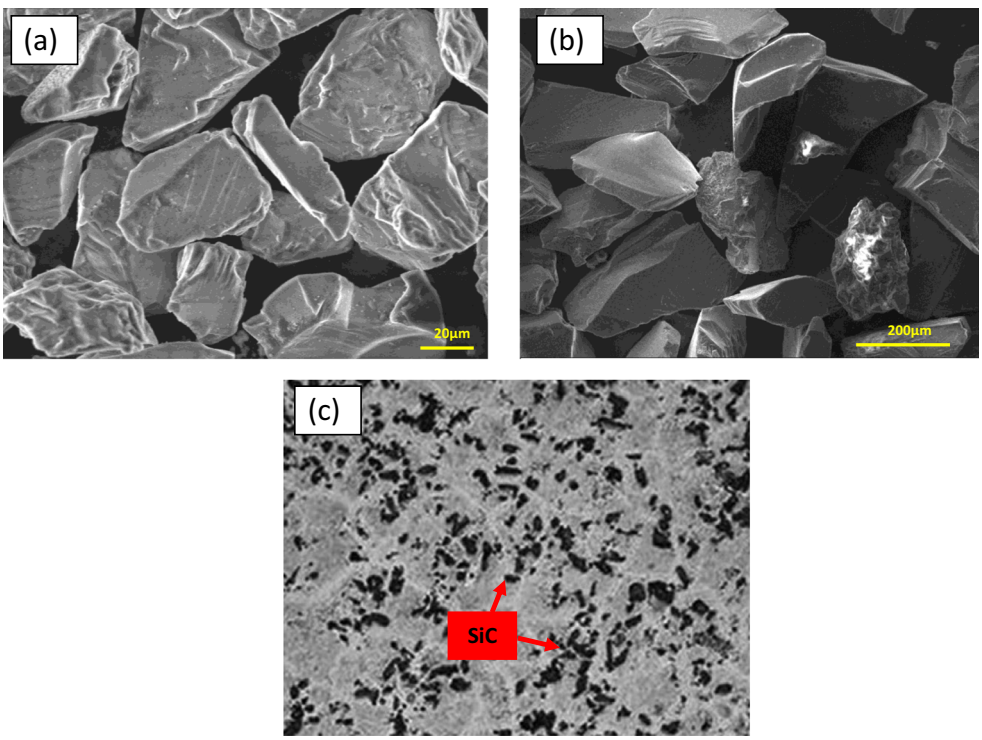

Fig. 1 **a** Erodent (Alumina) particles, (**b**) Reinforcement SiC particles, (**c**) Microstructure of Mg/SiC

Table 1 Experimental parameters and its levels

Machining Parameters	Symbols	Levels			Time (min)
		1	2	3	
Impact Angle (Deg)	IA	30	60	90	20
Erodent Velocity (m/s)	EV	41	72	100	20
Discharge (gms/min)	DR	2.5	3.3	4	20

under the argon atmosphere. 1200 g of Mg powder is heated to a temperature of 750 °C in the resistance furnace with an argon environment. SiC of particle size 23 μm is preheated to a temperature of 600 °C and it is slowly added into the corner of the vortex during stirring. Aluminium of 5% weight ratio is added into the vortex to improve the wettable of SiC particle. After continuous stirring for 5 min, the mixture is poured into the steel mold which was preheated to the temperature of 350 °C. Finally, the sample is sandblasted to remove the unwanted materials that stick over the surface. Further, to obtain uniform grain refinement, the composite is sintered at 400 °C for 4 h.

2.2 Experimental Procedure

Erosion wear tester of Ducom made TR470 model that has a nozzle diameter of 1.5 mm is used as the test machine to perform the erosion study. Alumina having the mesh size of 20–30 μm is used as the erodent material. Alumina and reinforced SiC particles are shown in Fig. 1(a&b). The uniform dispersion of the SiC particle in the matrix is shown in Fig. 1 (c). The samples are cut to ASTM Standard G76 (2013) and the size of the sample is 25 × 25 × 5 mm. The samples are cut to a specific geometry by using the abrasive waterjet machine. Before conducting the experimental study, the samples are polished to fine ground finish. The various operating parameters and levels are shown in Table 1. The output response of erosion rate in grams/ min is governed by the machining parameters likely: impact angle, erosion velocity and uniform discharge rate of alumina for a selected period of 20 min.

The erosion rate is measured by using the following eq. 1.

$$E_r = \frac{W_B - W_A}{t} \quad (1)$$

Where, E_r, W_B, W_A, and t are represented as erosion rate (gms/min), weight before machining (gms), weight after machining (gms) and time (sec), respectively.

Micro-Vickers hardness tester is used to measure the hardness on the impinged surface. Five different observations are taken on the impact region and the average of five observations is taken into consideration. The experimental arrangements of air jet erosion tester, fabricated sample and machined sample are shown in Fig. 2. The density of the composite is measured using the Archimedes principle. The theoretical and experimental density of the composite is measured to be 1.918 g/cm^3 and 1.862 g/cm^3, respectively. The porosity of the composite is calculated as 1.02 (in volume percentage).

To meet the required industrial standard and to get the accurate observations Taguchi's L27 orthogonal array (OA), a full factorial design experimental study is performed on Mg/SiC composites with different operating conditions. To

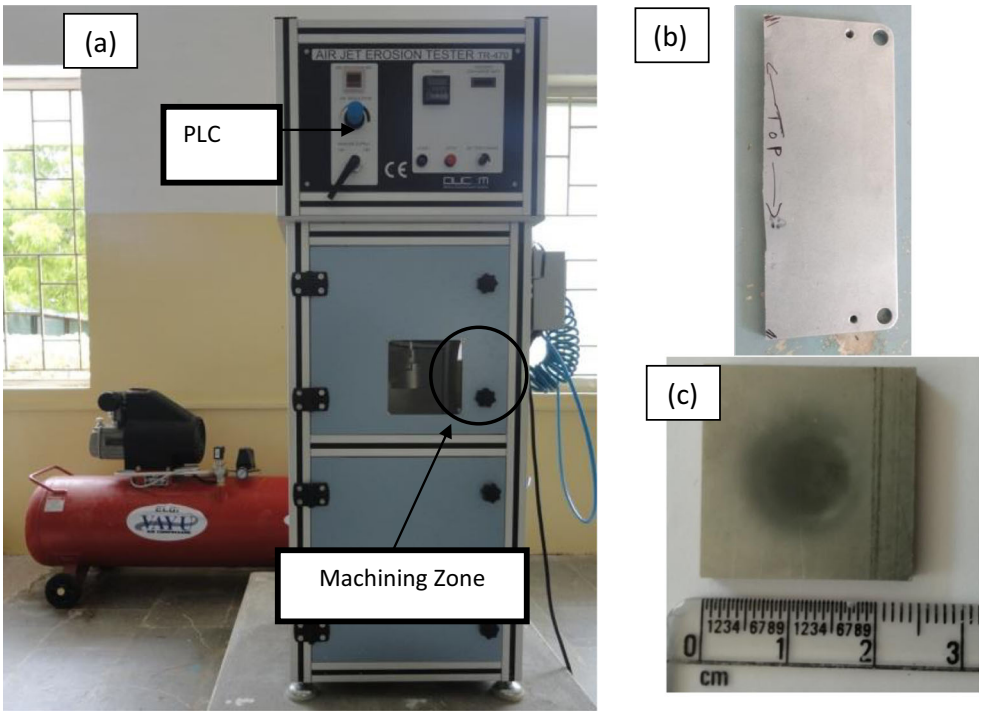

Fig. 2 **a** Experimental arrangement of air jet erosion, (**b**) Sample before machining and (**c**) Sample after machining

compute OA for 3 parameters with 3 levels, the required number of experimental runs can be computed from eq. (2)

$$1 + P(L-1) \quad (2)$$

Where P = Number of parameter and L = Total number of levels.

By using the eq. (2), a total of seven experimental runs are required. L9 OA (partial factorial design) a total of nine experimental runs is enough to examine Er for Mg/SiC composite. Here examining on the interaction effect of the machining parameters are not possible hence, it is always advisable to have a full factorial design that will have a total of twenty seven experimental runs (i.e) L27 OA. Table 2 shows L27 OA table with the machining parameters and the output responses. Computer assisted mathematical tool can be used for the given Table 2 to meet required needs and it will also helps in exploring more about the erosive property of Mg/SiC composite.

Table 2 Experimental observation of erosion test

S.NO	IA (Deg)	EV (m/s)	DR (gms/min)	Er $*10^{-3}$ (gms/min)	VHN
Unmachined surface					52.6
1	30	41	2.5	7.199	59.1
2	30	41	3.3	5.454	59.4
3	30	41	4	2.979	60.8
4	30	72	2.5	10.808	58.1
5	30	72	3.3	8.542	58.4
6	30	72	4	7.01	60.1
7	30	100	2.5	15.44	59.4
8	30	100	3.3	13.36	59.6
9	30	100	4	9.32	60.1
10	60	41	2.5	5.92	62.3
11	60	41	3.3	4.81	62.4
12	60	41	4	3.505	63
13	60	72	2.5	8.8	60.9
14	60	72	3.3	6.48	61.1
15	60	72	4	4.5	62.3
16	60	100	2.5	12.6	61.9
17	60	100	3.3	10.93	62.3
18	60	100	4	8.5	65.9
19	90	41	2.5	6.49	69.9
20	90	41	3.3	2.81	69.7
21	90	41	4	2.2	71.1
22	90	72	2.5	7.8	68.5
23	90	72	3.3	6.69	69.1
24	90	72	4	5.5	69.2
25	90	100	2.5	10.15	67.9
26	90	100	3.3	8.09	69.1
27	90	100	4	7.9	70.6

3 Results and Discussion

3.1 Analysis of Variance

ANOVA observation is shown in Table 3 to view the effect of the contribution of each machining parameter. Through the ANOVA observation, it can be confirmed that EV is having a significant contribution over the other parameters with the contribution of nearly 59% and followed by DR and IA with a contribution of 23% and 12%, respectively. The interaction effect of IA and EV has found an effective role in the erosion of Mg/SiC composite. High level of EV, irrespective of removing the materials, the action imports hardness on the machined surface is because the direct impingements on hard alumina on the composite creates a bouncing effect and induce hardness on the surface which could be clearly explained in the surface morphology section. The decrease in nozzle angle from 90° increases the sliding velocity of the erodent particles that leads to having superior surface erosion and creating the wear track over the surface. From Table 2, it can be stated that DR is having a less significant effect on erosion of composite at low nozzle angle.

3.2 Influences of Independent Parameters

The effect of every machining parameter on erosion tester has found to give a significant impact on machining the sample. To understand the influence of each independent parameter the interference chart is prepared by setting one parameter as constant and it is shown in Fig. 3. The increase in DR leads to the collision of alumina particles with the backscattered alumina particles. This action reduces the acceleration energy of the new alumina particles, this partial energy loss particles creates wear mark on the impinged region and increase the hardness on the machined surface. The aforesaid statement could be suitable when the nozzle is at an angle of 90°, a decrease in the angle of the nozzle allows the slippery effect to the hard alumina particles and hence the alumina particles slide over the surface of the composite creating the wear track all over the surface and cause erosion.

Table 3 ANOVA observation

Parameters	SS	DOF	MS	F-Value	Contribution %
IA	32.019	2	16.0097	46.10	12.26
EV	152.727	2	76.3635	219.93	58.48
DR	60.776	2	30.3883	87.52	23.27
IA x EV	8.404	4	2.1010	6.05	3.21
IA x DR	2.260	4	0.5651	1.62	0.86
EV x DR	2.185	4	0.5462	1.57	0.83
Error	2.777	8	0.3473		1.06
Total	261.151	26	125.974		100

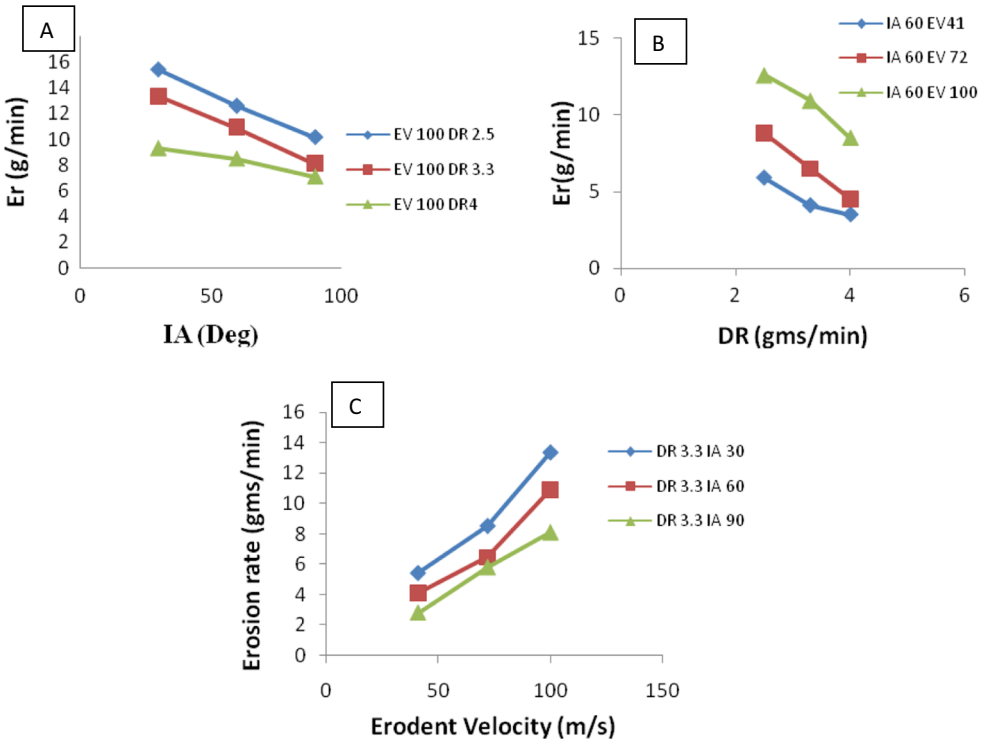

Fig. 3 Interference chart of machining parameter. **a** Er vs (IA & DR), (**b**) Er vs (DR & EV), (**c**) Er vs (EV & IA)

Bata et al. [17] report on solid particles erosion in Ti6Al4V is found to have a similar effect like Mg/SiC composite. The impact angle greatly determines the surface profile of the composite. Further, maximum erosion occurs at the low impact angle with the ductile type plastic deformation failures on the surface and it could be verified from Fig. 3(a). From Fig. 3(b) there is a steady fall with an increase in DR is observed and it is due to the high discharge of alumina particles improves the hardness of the surface rather than performing the erosion operation at high nozzle angle. Avcu et al. [18] reported that on solid-state erosion test, an increase of erodent discharge creates more wear track all over the machined surface is due to the collision of the erodent particles and have low materials removal rate. From Fig. 3(c), it can be stated that EV has a more significant effect on the erosion of the composite material. From the observation, it is noticed that half the increment in EV will lead to almost double the erosion rate. Kaplan et al. [19] stated that improvement in sliding velocity of the erodent particles removes the maximum amount of materials at the nozzle angle of 60°.

Figure 4 shows the plot between SN and levels of each machining parameter. From Fig. 4, it could be confirmed that all the three machining parameters (IA, EV, and DR) have its individual effect on output response. However, based on the angle of slope, EV has a higher degree angle than the rest which indicates that it should be the most significant machining process parameters on the output response. DR and IA have found to be the next successive influential factors. The

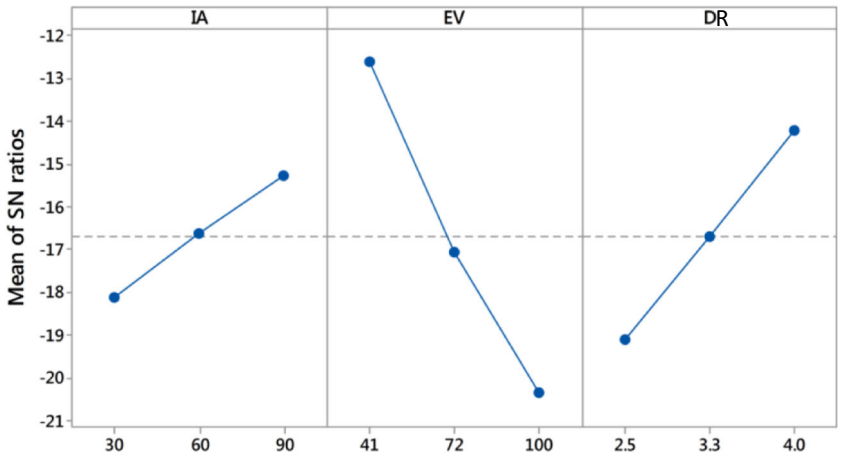

Fig. 4 SN plot on erosion observations

contribution of EV, DR and IA are 59%, 23%, and 12%, respectively. Through the Fisher Table (F-table), the interaction between IA and EV has found to have a significant effect on the output response with the contribution of 3.2%.

3.3 Analysis of Surface Profile Parameters

To examine the surface profile of the machined composite material, 3-D optical study is performed by capturing the images on the eroded surface and it is shown in Fig. 5. According to Sedacek et al. [20], superior observation on Sku is due to the low friction that is observed between the contact surfaces. Similar kind of observation is noticed at all images shown in Fig. 5 (a-e) with a change in the orientation of the nozzle. The maximum Sku value of 11 μm is observed at the nozzle angle of 30°. By means of observing the Sp (Peak) value, it could be possible to say that the gradual decrement occurs with the decrease of IA and this is because of the uniform flow of alumina particles over the surface irrespective of DR.

Owing to the low friction at the low IA, the forged alumina leaves behind the wear mark and erodent of some composite material from the top surface and is shown in Fig. 5(c) imaged at a nozzle angle of 60°. It is believed that the newly entered alumina particles are allowed to pass through the root region of the peaks which are generated during the erosion process at the earlier stage. The effect of the discharge rate of the alumina

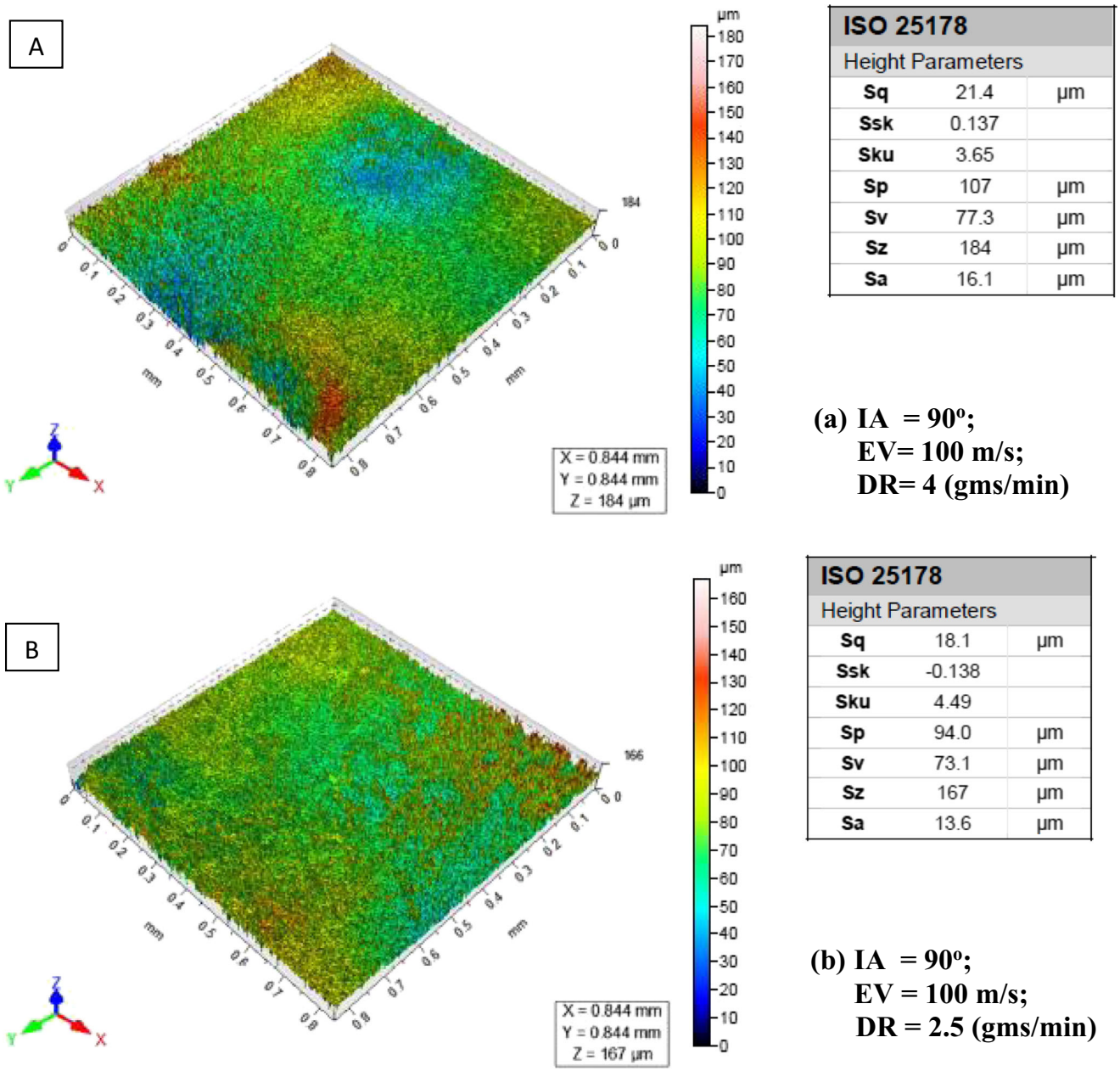

Fig. 5 3D optical images on the machined surface at various operating conditions

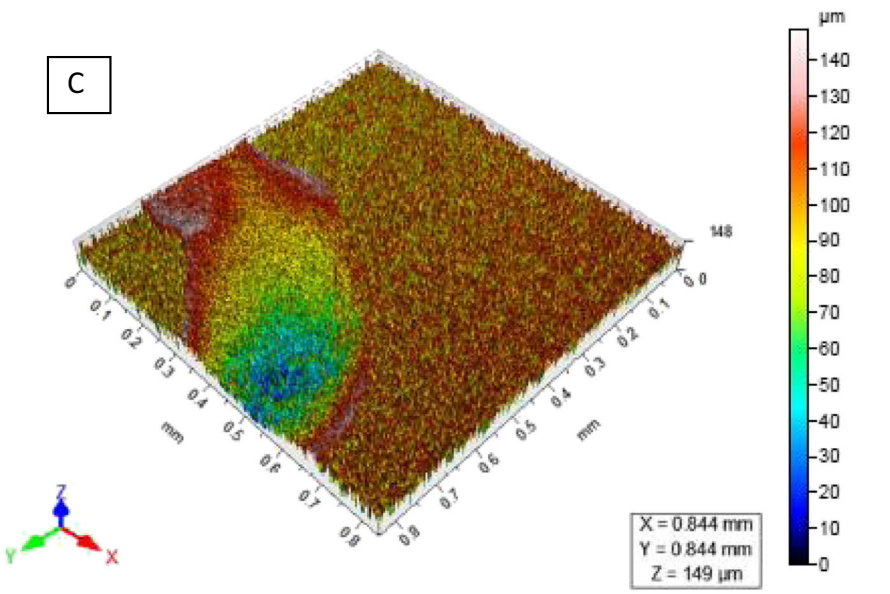

ISO 25178		
Height Parameters		
Sq	29.4	µm
Ssk	-0.0681	
Sku	2.31	
Sp	65.2	µm
Sv	83.6	µm
Sz	149	µm
Sa	24.4	µm

(c) IA = 60º; EV= 100 m/s; DR= 4 (gms/min)

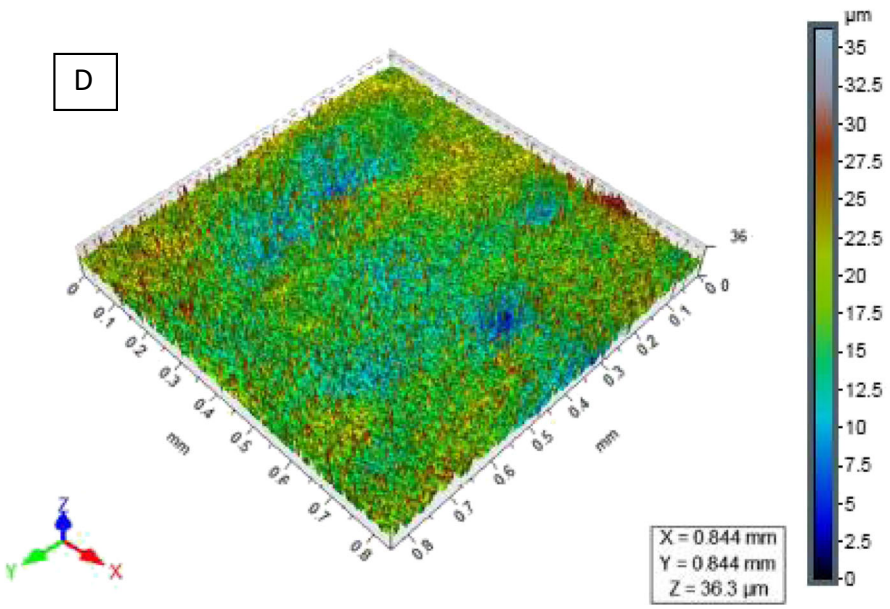

ISO 25178		
Height Parameters		
Sq	4.72	µm
Ssk	0.411	
Sku	7.75	
Sp	21.2	µm
Sv	15.0	µm
Sz	36.3	µm
Sa	3.19	µm

(d) IA = 30º; EV= 100 m/s; DR= 2.5 (gms/min)

Fig. 5 (continued)

could be clearly noted in Fig. 5(d&e), the Sp and Sv values are found to have similar observations at IA of 30°. It is clear to confirm that the surface is free from peaks and valleys. Hence, lower IA and high DR will enhance the machining surface roughness irrespective of the increase in hardness.

Ssk values in all the images shown are found to be greater than three (>3) signifies that the surfaces formed consists of more numbers of peaks above the mean value. Xie and Rittel [21] could able to get negative skewness (Ssk) on waterjet peening stating that most of the peaks are blended through high-pressure water. Similar kind of observation is observed while machining Mg/SiC composite at a high discharge rate.

3.4 Surface Morphological Studies

Figure 6 depicts the surface morphologies of worn surfaces of tested specimens at impact angles of 90°, 60° and 30°. It is evident that the surface characteristics or nature of craters formed by alumina particles vary with different impact angles (compare Fig. 6(a&c)). This can also be supported by surface roughness profiles of the eroded specimen as illustrated in Fig. 5. For instance, both the size and depth of craters in samples impacted at an angle of 60° is relatively large when compared to specimens with particle impact angles of 30° and 90°.

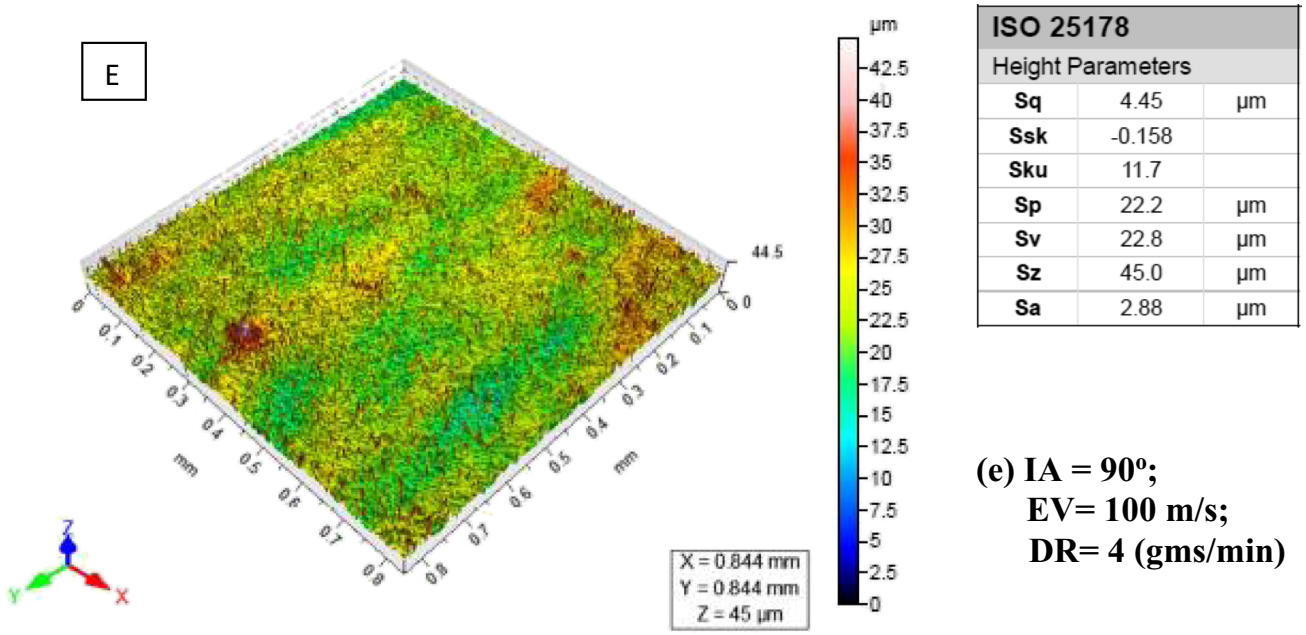

Fig. 5 (continued)

Such a difference in surface morphologies is associated with variation in the degree of plastic deformation takes place at the eroding specimen.

In Fig. 6(a&b), the impact of alumina particles normal (impact angle of 90° with the varied DR) to the worn surface results in significant plastic deformation featured by wavy patterns with craters and dimples. The amount of material removal rate is found to be considerably low at the high angle signifies that instead of eroding the surface, the impact of hard alumina particles induced hardness on the surface of the composite and this could be confirmed through the Table 2. Chowdhury et al. [22] experimental study on the erosion of mild steel experiences similar behaviour at high impact angle especially at 90°. For specimen with an impact angle of 60°, the worn surface analysis showed the mixed modes of brittle and ductile erosive wear. The increase of wear rate between the alumina particles and the composite surface is found to be excellent at this angle. This enhances the excess loss of material and creates a deep crater at the impact region and this could be verified from Fig. 6(c&d). The specimen with an impact angle of 60° reveals the cleavage pattern represented by a large number of micro-cracks as indicated in Fig. 6(e&f). Several cracks are initiated along the edge of the reinforced SiC particle is due to the decohesion bond between the magnesium matrix and SiC particles and it is shown in Fig. 6(f). Srinivasa [23], confirms that microstructure generated on solid erosion test will be in the form of micro-cutting or micro-ploughing that leads to micro cracks on the machined surface.

Figure 6(g&h), it is predicted that the lower impingement angle leads to form high peaks (crater lip) and this is due to the larger number of wear tracks created by the irregular shaped alumina particles. The sliding action of the abrasive, irrespective of removal of materials through erosion, it also induces some hardness over the surface of the composite and this could be confirmed with the reduction of peak heights. Alam and Farhat, [24] stated that the energy induced on the surface of the samples by erodent with a low impact angle created plastic deformation platelets on the eroded zone. A similar observation is noticed on the machined samples of Mg/SiC composite. From Table 2, it can be observed that erosive wear of magnesium matrix composites reinforced with SiC particles increased with decreasing in IA. Our experimental observation indicates that more amount of material can be easily removed at low impact angles. The erosive phenomenon is dominated by micro-cracking and spalling mechanisms whereas material removal rate is very limited at high impact angle. Material experiences a significant amount of plastic deformation akin to ductile materials. This experimental data is quite consistent with the statement given by Hutchings, [25].

4 Conclusion

Mg/SiC is successfully prepared through a stir casting process. The obtained samples are cut to the required dimensions. The specimens are subjected to air jet erosion with alumina as erodent. The experiments are performed and the following conclusions are drawn.

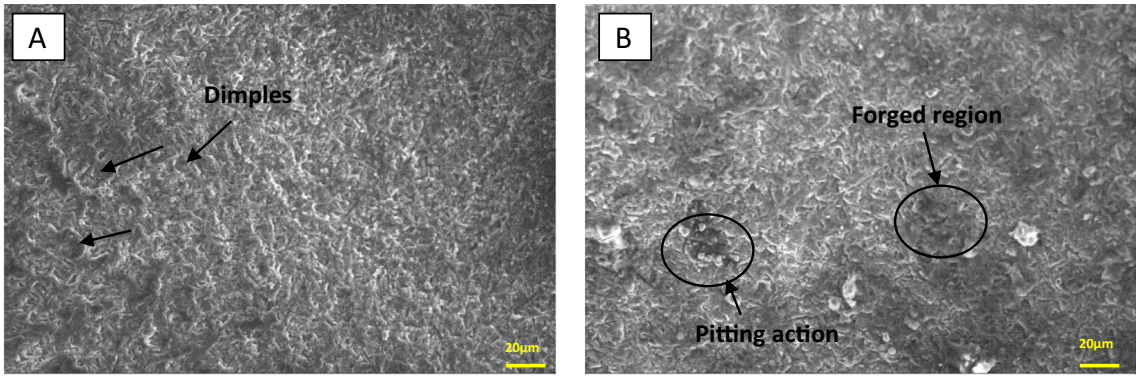

(a) IA= 90°; EV=100; DR=2.5

(b) IA= 90°; EV=100; DR=4

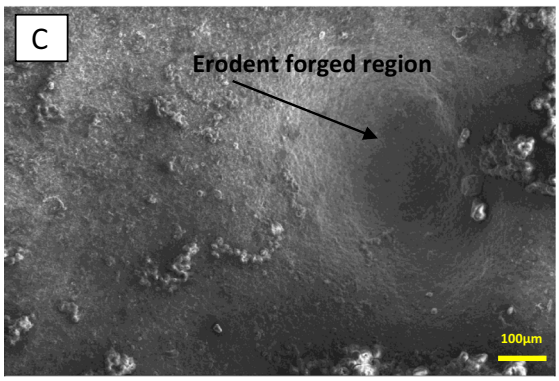

(c) IA= 60°; EV=100; DR=2.5

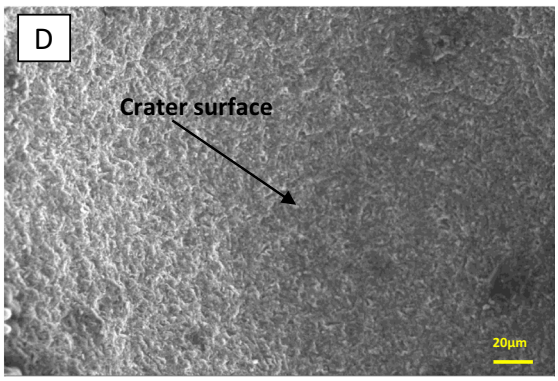

(d) Crater surface profile

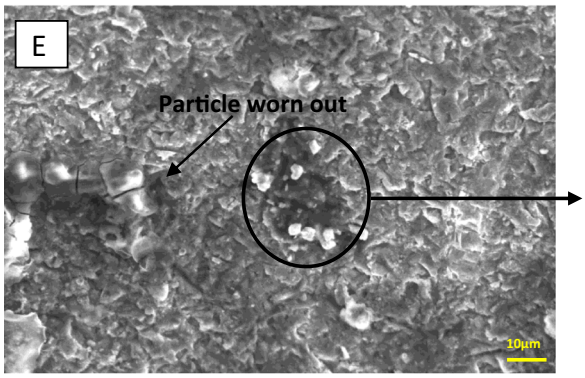

(e) IA= 60°; EV=100; DR=4

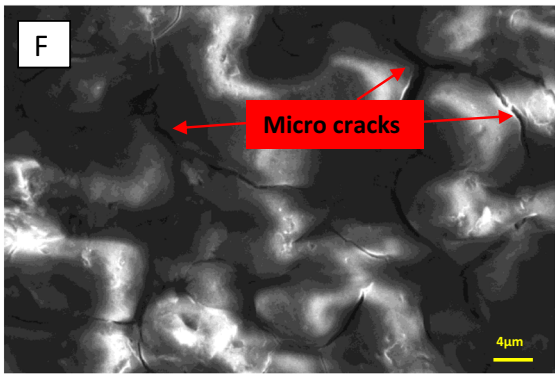

(f)) Forged region

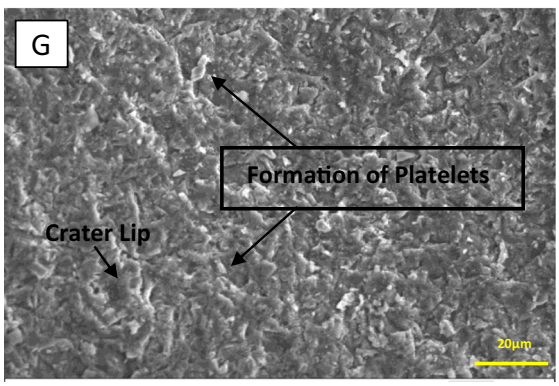

(g) IA= 30°; EV=100; D=2.5

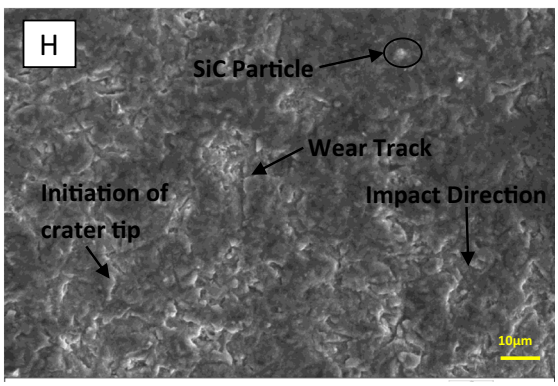

(h) IA= 30°; EV=100; D=4

Fig. 6 Surface image of the machined sample at various operating conditions

- When the nozzle is placed normal to the sample and at high DR, the impinged alumina increases the hardness of the materials with least erosion rate.
- With the decrease of nozzle angle from 90° to 30°, the increase in wear rate is recorded. Plastic deformation surface is formed due to the impact of the hard alumina particles.
- ANOVA observation reveals that irrespective of IA, EV is found to have a significant contribution of nearly 59%, and followed with DR and IA with a contribution of 23% and 12%, respectively. The interaction effect of IA and EV has found an effective role in the erosion of Mg/SiC composite with the contribution of 3.2%.
- By understanding the effect of machining parameters it can be stated that half the increment in EV progressed towards doubling the erosion rate.
- The decrease in nozzle angle increase the slippery of the alumina particles on the surface and leads to incremental erosion rate and this could be verified by the surface profile parameter like Sku skewness.
- All the machined surfaces have the least value of Ssk reveals that the surface is full of peaks with the value more than the mean. The surface defect is found to be superior at the nozzle angle of 60°.
- Plastic deformation surfaces with micro-cracking and spalling mechanisms are found at all considered nozzle angle. A significant amount of plastic deformation akin to ductile materials low erosion rate is recorded for 90°, a mixed mode of brittle and ductile erosive wear is observed at 60° and at 30°, due to the excess amount of flow of materials over the surface leads to small peak heights.

References

1. Viswanath A, Dieringa H, Ajit Kumar KK, Pillai UTS, Pai BC (2015) Investigation on mechanical properties and creep behavior of stir cast AZ91-SiCp composites. J Magnes Alloy 3:16–22
2. Kumar PS, Viswanath A, Ajith Kumar KK, Rajan TPD, Pillai UTS, Pai BC (2013) Sliding Wear behavior of stir cast AZ91/ SiCp composites. J Solid Mech Mater Eng 7:169–175
3. Vishwas DK, Chandrappa CN, Venkatesh S (2018) Study on erosion behaviour of hybrid aluminium composite. AIP Conf Proc 1943:020121
4. Gousia V, Tsioukis A, Lekatou A, Karantzalis AE (2016) Al-$MoSi_2$ composite materials: analysis of microstructure, sliding Wear, solid particle Erosion, and aqueous corrosion. J Mater Eng Perform 25: 3107–3120
5. Patel M, Patel D, Sekar S, Tailor PB, Ramana PV (2016) Study of solid particle Erosion behaviour of SS 304 at room temperature. Procedia Technology 23:288–295
6. Sharma SK, Kumar BVM, Kim YM (2017) Effect of impingement angle and WC content on high temperature erosion behavior of SiC-WC composites. Int J Refract Met Hard Mater 68:166–171
7. Khan MM, Dixit G (2017) Abrasive Wear characteristics of silicon carbide particle reinforced zinc based composite. Silicon 10:1315–1327
8. Mamatha TG, Patnaik A, Biswas S, Kumar P (2011) Finite element modelling and development of SiC-filled ZA-27 alloy composites in erosive wear environment: a comparative analysis. Proc Inst Mech Eng Part J J Eng Tribology 225: 1106–1120
9. Chowdhury MA, Debnath UK, Nuruzzaman DM, Islam MM (2015) Experimental evaluation of erosion of gunmetal under asymmetrical shaped sand particle. Adv Tribal 215:1–31. https://doi.org/10.1155/2015/815179
10. Rosa CSL, Vite-Torres M, Gallardo-Hernandez EA, Laguna-Camacho JR, Godinez-Salcedo JG, Farfan-Cabrera LI (2017) Effect of tangential velocity on erosion of ASTM A-106 grade B steel pipe under turbulent swirling impinging jet. Tribol Int 113: 500–506
11. Khan MM, Dixit G (2019) Evaluation of microstructure, mechanical, thermal and erosive Wear behavior of aluminum-based composites. Silicon. https://doi.org/10.1007/s12633-019-00099-4
12. Miyazaki N (2016) Solid particle erosion of composite materials: a critical review. J Compos Mater 50:1–43. https://doi.org/10.1177/0021998315617818
13. Yang JZ, Tsioukis A, Lekatou A, Karantzalis AE (2016) Al-$MoSi_2$ composite materials: analysis of microstructure, slding wear, solid particle erosion, and aqueous corrosion. J Mater Eng Perform 25: 3107–3120
14. Ruslan M, Fengzhou F (2019) Investigation of erosion temperature in micro-blasting. Wear 420/421:123–132. https://doi.org/10.1016/j.wear.2018.12.073
15. Krolczyk GM, Krolczyk JB, Maruda RW, Legutko S, Tomaszewski M (2016) Metrological changes in surface morphology of high-strength steels in manufacturing processes. Measurement 88:176–185
16. Krolczyk GM, Maruda RW, Krolczyk JW, Nieslony P, Wojciechowski S, Legutko S (2018) Parametric and non-parametric description of the surface topography in the dry and MQCL cutting conditions. Measurement 121: 225–239
17. Bata E, Lentzaris K, Lekatou AG, Barkoula NM, Poulia A (2017) Effect of solid particle Erosion on the aqueous corrosion behaviour of a Ti6Al4V sheet. Mater. Sci. Eng. Adv. Res 26–33 https://doi.org/10.24218/msear.2017.4S, Special Issue
18. Avcu E, Fidan S, Yıldıran Y, Sınmazcelik T (2013) Solid particle erosion behaviour of Ti6Al4V alloy. Tribol Mater Surf Interfaces 7: 201–210
19. Kaplan M, Uyaner M, Avcu M, Avcu YY and Karaoglanli AC (2018) Solid particle erosion behavior of thermal barrier coatings produced by atmospheric plasma spray technique, Mech Adv Mater Struct, https://doi.org/10.1080/15376494.4712018.1444221
20. Sedlacek M, Gregorcic P, Podgornik B (2017) Use of the roughness parameters Ssk and Sku to control friction—a method for designing surface texturing. Tribol Trans 60: 260–226
21. Xie J, Rittel D (2018) The effects of waterjet peening on a random-topography metallic implant surface. Eur J Mech A Solids 71:235–244
22. Chowdhury MA, Debnath UK, Nuruzzaman DM, Islam MM (2015) Erosion of mild steel for engineering design and applications. J. Bio-Tribo-Corros 3:34–51. https://doi.org/10.1007/s40735-017-0094-z

23. Srivastava VK (2006) Effects of wheat starch on erosive wear of E-glass fibre reinforced epoxy resin composite materials. Mater Sci Eng A 435/436:282–287
24. Alam T, Farhat ZN (2017) Slurry erosion surface damage under normal impact for pipeline steels. Eng Fail Anal 90:116–128. https://doi.org/10.1016/j.engfailanal.2018.03.019
25. Hutchings IM (1992) Tribology: friction and Wear of engineering materials. Edward Arnold, UK